Received: 22 December 2022 | Revised: 28 May 2023 | Accepted: 19 June 2023

DOI: 10.1002/jms.4957

RESEARCH ARTICLE

Journal of MASS SPECTROMETRY WILEY

Optimum collision energies for proteomics: The impact of ion mobility separation

Kinga Nagy[1,2] | Gabriella Gellén[3] | Dávid Papp[2,3] | Gitta Schlosser[3] | Ágnes Révész[1]

[1]MS Proteomics Research Group, Research Centre for Natural Sciences, Budapest, H-1117, Hungary

[2]Hevesy György PhD School of Chemistry, Faculty of Science, Institute of Chemistry, Eötvös Loránd University, Budapest, H-1117, Hungary

[3]MTA-ELTE Lendület Ion Mobility Mass Spectrometry Research Group, Faculty of Science, Institute of Chemistry, Eötvös Loránd University, Budapest, H-1117, Hungary

Correspondence
Ágnes Révész, MS Proteomics Research Group, Research Centre for Natural Sciences, Magyar Tudósok körútja 2., H-1117, Budapest, Hungary.
Email: revesz.agnes@ttk.hu

Funding information
Funding from the National Research, Development and Innovation Office (NKFIH PD-132135, FK-138678, and SNN 138407) is gratefully acknowledged. This project was supported by the Lendület (Momentum) Program of the Hungarian Academy of Sciences (HAS, MTA) and by the ELTE Thematic Excellence Programme Synth+, supported by the Hungarian Ministry for Innovation and Technology. Project No. 2018-1.2.1-NKP-2018-00005 has been implemented with the support provided from the National Research, Development and Innovation Fund of Hungary, financed under the 2018-1.2.1-NKP funding scheme.

Abstract

Ion mobility spectrometry (IMS) is a widespread separation technique used in various research fields. It can be coupled to liquid chromatography–mass spectrometry (LC–MS/MS) methods providing an additional separation dimension. During IMS, ions are subjected to multiple collisions with buffer gas, which may cause significant ion heating. The present project addresses this phenomenon from the bottom-up proteomics point of view. We performed LC–MS/MS measurements on a cyclic ion mobility mass spectrometer with varied collision energy (CE) settings both with and without IMS. We investigated the CE dependence of identification score, using Byonic search engine, for more than 1000 tryptic peptides from HeLa digest standard. We determined the optimal CE values—giving the highest identification score—for both setups (i.e., with and without IMS). Results show that lower CE is advantageous when IMS separation is applied, by 6.3 V on average. This value belongs to the one-cycle separation configuration, and multiple cycles may supposedly have even larger impact. The effect of IMS is also reflected in the trends of optimal CE values versus *m/z* functions. The parameters suggested by the manufacturer were found to be almost optimal for the setup without IMS; on the other hand, they are obviously too high with IMS. Practical consideration on setting up a mass spectrometric platform hyphenated to IMS is also presented. Furthermore, the two CID (collision induced dissociation) fragmentation cells of the instrument—located before and after the IMS cell—were also compared, and we found that CE adjustment is needed when the trap cell is used for activation instead of the transfer cell. Data have been deposited in the MassIVE repository (MSV000090944).

KEYWORDS
bottom-up proteomics, collision energy, cyclic ion mobility mass spectrometry, ion mobility separation, peptide identification

1 | INTRODUCTION

Ion mobility spectrometry (IMS) has become a widespread separation technique in analytical and physical chemistry, often hyphenated to mass spectrometric (MS) analysis ("IM-MS"). IMS separation occurs in the millisecond timescale; therefore, it can be easily incorporated into the conventional liquid chromatography–mass spectrometry workflows (LC–MS/MS) and can further boost the performance by providing a dimension for separation that is complementary to the usual chromatographic techniques.[1,2] IM-MS has found applications in various scientific areas from metabolomics[3] through characterization of lipids[4] and nucleic acids[5] to the structural analysis of polymer mixtures[6] and artificial molecular machines.[7] It is also a useful tool in protein chemistry and proteomics, providing information on protein conformations and unfolding processes,[8,9] as well as increasing the peak capacity and therefore the number of peptide identifications in bottom-up studies.[10–12]

Ion mobility is based on the transport of ions in buffer gas under the influence of an electric field and separates species by charge state and shape, and the latter is characterized by collision cross section (CCS). IM-MS can provide the measurement of CCS either directly or with the help of calibration to reference compounds of known CCS values.[2,13,14] IMS methods are used in various ways in the field of proteomics, such as for separation of isomers having similar structures, for signal filtering to reduce complexity of MS measurements, for aiding identification via mobility related values (e.g., CCS) in proteomics experiments, and for gaining insight into the conformational dynamics of a system.[15–18] During mobility separation, the peptide ions are pushed through a buffer gas by electric field while collisions with the buffer gas hamper their motion. The most conventional drift tube IMS (DTIMS) operates in the condition of low-field limit (low *E/N*, low electric field to gas number density ratio), where the ion velocity in the direction of electric field is negligible compared to the thermal velocity and the effective ion temperature is equal to the temperature of the buffer gas.[19] However, most commercial IMS setups, such as traveling wave IMS (TWIMS), trapped ion mobility spectrometry (TIMS), and field asymmetric waveform IMS (FAIMS), work with much larger *E/N* ratio,[20–22] where the ion drift velocity is greater than its thermal velocity. This approach raises questions regarding the temperature of ions under study and the possibility of ion heating upon IMS experiments.[19]

The ions are subject to a series of collisions in the IMS cell, and a fraction of their kinetic energy can be transferred to internal energy via inelastic collisions. The obtained energy is then distributed among rotational and vibrational degrees of freedom; hence, the activation of the ions takes place similar to collision-induced dissociation (CID).[23] As internal energy increases because of the frequency of collisions, conformational changes, structural rearrangements, and fragmentation processes can occur.[19,23,24]

These phenomena can affect both the distributions of conformations and the CCS determination[24–26] as well; therefore, the qualitative and quantitative measure of ion heating during IMS separation is of significant importance, and several studies addressed this issue.[19,23–35] There are several instrument platforms to carry out mobility separation, and because of the differences, the magnitude of ion heating can be also different; even different members of the same instrument series may show variances.[26,28,30] The investigations revealed that the major influencing experimental parameters are wave height, wave speed, and injection voltage to the IMS cell for TWIMS setups,[19,20,24,31] while the series of transfer DC potentials altering transmission and the RF amplitude are critical for TIMS mass spectrometers.[18,26,32–34] Greater ion heating occurs at lower pressures, and the transfer efficiency of argon is higher than for He, N_2, or CO_2; therefore, optimal parameters may be dependent on the buffer gas.[19,23–25,31,32,35] While the pressure dependence seems contraintuitive, it has been observed consistently in multiple independent experimental setups.[19,24,32] Qualitatively, decreasing the pressure, thereby the density, leads to fewer collisions, but the drift velocity is increasing, which leads to an even faster increase in the collision energy (CE) that can be transferred.[19,24,32] Analysis timescale for TIMS equipment and prestore time for cyclic TWIMS also count.[26,27] Further, the process is also dependent on the species under study: larger ions are less heated as the extent of collisional activation per degree of freedom should decrease with ion size and higher charged states are activated more than lower charged ones.[19,23,25,27,29,32,34,36] Even the solvent used for electrospray ionization (ESI) and microsolvation of gas phase ions may have an effect.[35,37] The existence and magnitude of ion heating were determined applying the survival yield method on thermometer ions (e.g., p-substituted-benzylpyridinium ions and leucine enkephalin),[19,24–26,29,32] investigating the dissociation of fragile compounds (e.g., leucine enkephalin dimer and DNA G-quadruplex)[25,35,38] and studying the conformer distribution of proteins (e.g., bradykinin, ubiquitin, myoglobin, lysozyme, and cytochrome c).[18,23,25–27,32,34,35] The values obtained for effective temperature ranged from ~400 K to 800 K depending on the instrument, on the experimental parameters, and on the investigated species. It was also shown that the native structure of the proteins can be preserved by the careful tuning of measurement settings.[18,26,27,32,33,35,36]

Despite the detailed investigation of ion heating process in IMS cell, no one has yet studied the impact of ion mobility separation on peptide ion energetics from the point of view of peptide identification and thereby on the optimal CE choice of MS/MS experiments. In bottom-up proteomics, peptides are typically subjected to tandem mass spectrometric experiments and then are identified through matching their MS/MS spectra against theoretical spectra formed from a sequence database. One of the most widely used fragmentation technique is CID, where the applied CE has profound impact on the information content of the obtained MS/MS spectra. In particular, this phenomenon has been widely documented from practical proteomics aspects for both unmodified peptides[39,40] and peptides with post-translational modifications.[41–47] It was shown to be important to use instrument specific optimal setting to achieve best proteomics performance in terms of identification scores and number of successful identifications.[40,48,49]

The present study focuses on the influence of the application of IMS on the optimum CE at the individual peptide level for a large number of peptides. Various commercial IMS instruments have been

developed in the last few decades. The present project was carried out on the state-of-the art Waters Select Series Cyclic IMS, which consists of a 98 cm path length, closed-loop traveling wave (TW)-enabled IM separator positioned orthogonally to the main ion optical axis. This configuration enables multiple-pass experiments and provides a very powerful platform when high-resolution separation is desired.[50,51] The investigation of polycyclic aromatic hydrocarbons showed an almost doubled resolving power by allowing three passes in the circular TW.[52] For intact protein complexes, increased mobility resolution by an average of 15% per pass was observed.[53] Separation of oligosaccharides resulted in a resolving power of approximately 120 using three passes,[54] while an estimated resolution of 920 could be achieved after 58 cycles.[55] Because of its outstanding efficiency, cyclic IMS was applied in various proteomics studies as well, both for peptide[56–62] and protein[27,63–69] analysis. This technique was shown to provide more identified peptides resulting in increased sequence coverage.[56] It was used to map ligand binding sites,[56] to differentiate isobaric synthetic peptides derived from biopharmaceuticals,[57] and to unambiguously assign the disulfide bonds of therapeutic mAb peptides.[58] Further, cyclic IMS was found beneficial in the investigation of modified peptides to determine site localization (e.g., phosphorylation[59] or aspartic acid isomerization[60]) and to unravel linkages in glycosylation.[61,62] Incorporation of cyclic IMS in the intact protein identification led to improved number of proteins detected from tissue samples.[63] Top-down ECD approach combined with cyclic IMS could increase the number of fragment ions and protein sequence coverage.[64] It was demonstrated that cyclic IMS efficiently separates protein conformers[65,66] and is capable to monitor the extent of protein unfolding.[67,68] Further, protein conformational changes may occur upon (multipass) cyclic experiments depending on the voltage settings applied.[27,69]

Establishing that cyclic IMS is indeed a highly relevant platform for our investigations, our aim with the present project is to formulate practical suggestions on choosing the best CE setting for proteomics if IMS is used. In this article, we thus present the investigation of CE dependence of peptide identification scores for a large number of individual peptides both with and without the application of IMS and provide the comparison of the obtained results. To this end, we performed LC–MS/MS measurements on the commercially available HeLa tryptic digest standard with varied CE values using a Waters Select Series Cyclic IMS mass spectrometer. The applied equipment has two consecutive CID cells: one before and one after the ion mobility cell. Therefore, we could additionally compare the pre- and post-ion mobility fragmentation modes. Our results contribute to fully exploiting the performance boost of the IMS-MS coupling in the field of proteomics.

2 | EXPERIMENTAL SECTION

2.1 | Chemicals and reagents

LC–MS grade solvents and formic acid (FA) were from VWR International (Debrecen, Hungary), whereas HeLa tryptic digest standard was purchased from Thermo Fisher Scientific (Thermo Fisher Scientific, Waltham, MA, USA). Leucine enkephalin, MassPREP™ enolase digestion standard, and [Glu1]-Fibrinopeptide B were obtained from Waters (Waters Corporation, Milford, MA, USA).

2.2 | Mass spectrometry analysis

In each run, 200 ng HeLa tryptic digest standard reconstituted in 2% acetonitrile (ACN) + 0.1% formic acid (FA) (*V*/*V*) solution was injected onto a Waters Acquity I-Class UPLC system connected to Waters Select Series Cyclic IMS (Waters Corporation, Milford, MA) equipped with a low flow ESI source. Peptides were separated on Waters Acquity Premier CSH column (150 mm × 1 mm, 1.7 µm) at 45°C using multi-step gradient elution with a flow rate of 20 µL/min. Solvent A was 0.1% FA in water, whereas solvent B was 0.1% FA in ACN. The elution method was as follows: 5% B from 0 to 1 min, followed by a 44 min gradient to 35% B, then the ratio of the solvent B was elevated to 85% in 1 min and decreased to 5% in 5 min. The capillary and cone voltages were set to 2.7 kV and 40 V, respectively, whereas the source offset was 10 V. The source and desolvation temperatures were kept at 120°C and 400°C, respectively. The flow rates of the cone and the desolvation gases were 20 L/h and 800 L/h, respectively. The nebulizer gas pressure was 6 bar.

MS/MS measurements were recorded on a Waters Select Series Cyclic IMS QTof instrument. Data acquisition was performed in the *m/z* range of 50–2000 in V-mode. Scan time was set to 0.5 s, and single lock mass correction was carried out using leucine enkephalin. Collision energy was varied along the experimental series (see section 2.2.1). Further parameters are presented in the supporting information (see Table S1).

2.2.1 | Energy-dependence studies

We analyzed the CE dependent fragmentation behavior of tryptic peptides and determined the peptide level optimal CE values. The Waters Select Series Cyclic IMS mass spectrometer involves two CID cells; there is one before the IMS cell called "trap cell" and another one is located after the IMS cell called "transfer cell" (see Figure 1). Four energy-dependent experimental series were recorded combining the two fragmentation modes (i.e., trap or transfer) and the presence of mobility separation (i.e., with or without IMS). The measurements mapped the 10 to 60 V CE range in 2 V steps in 26 separate LC–MS/MS runs. While the CE was varied systematically in one of the collision cells, the CE was kept at the default low-energy value in the other collision cell. The default low-energy setting is 4 and 6 V for the transfer cell and the trap cell, respectively. The manufacturer's original suggestion for a default MS^E and $HDMS^E$ ramp setting was 19–45 V; the scanned range was chosen to broaden it in both directions. In the case of scanning the trap CE, discrete CE values were set. In the case of mapping transfer CE, it was not possible to set one value in the software; therefore, small ramps of 2 V were used. These measurements are marked with the average of the starting and ending settings

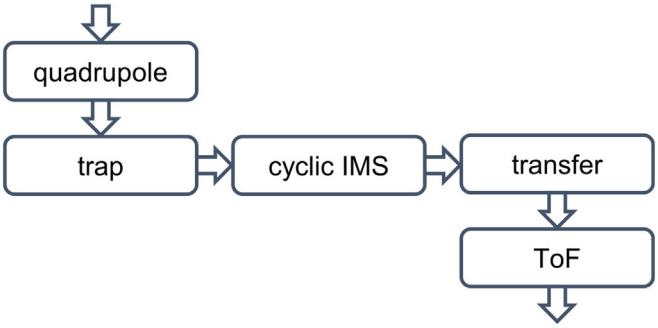

FIGURE 1 The schematic block diagram of the Waters Select Series Cyclic IMS QTof instrument. Activation can be initiated in the "trap cell" before the IMS cell and in the "transfer cell" after the IMS cell. Therefore, both pre- and post-ion mobility fragmentation can be carried out and a comparison between the two options can be made. IMS, ion mobility spectrometry.

for the sake of simplicity (e.g., 11 indicates the ramp of 10–12 V). For ion mobility separation, the default parameters of the one-cycle separation were applied. Experimental parameters are summarized as a form of screenshots in Figures S1–S9).

2.3 | Data analysis

The raw experimental data of Waters Select Series Cyclic IMS QTof mass spectrometer were converted to the mzML file format using Waters ProteinLynx Global Server 3.0.3 (PLGS) software. Then, MS/MS spectra were searched against the human SwissProt (February 2022) database using PLGS and Byonic search engines. The common parameters were as follows: trypsin as the enzyme, cysteine carbamidomethylation as fixed modification, and one missed cleavage allowed.

2.3.1 | PLGS search

Database search was performed using the 3.0.3 version of PLGS search engine (Waters). Parent and fragment ion tolerance was set to 20 and 30 ppm, respectively. Methionine oxidation was selected as variable modification. The false discovery rate was set to 1%. The processing parameters were set as follows: low energy threshold value: 200 counts, high energy threshold value: 20 counts, minimum fragment ion matches per peptide: 3, minimum fragment ion matches per protein: 7, and minimum peptide matches per protein: 1. We only accepted peptide identifications that exceeded a minimum score requirement of 5.[70]

2.3.2 | Byonic search

We employed Byonic v4.2.10 (Protein Metrics, Cupertino, CA) for our analysis. Byonic cannot handle the ion mobility data provided by the Waters instrument; therefore, the mzML files generated by PLGS were used. Regarding mass tolerance values, the same settings were applied as for the PLGS search. Byonic allows the handling of more variable modifications compared to conventional database searches because of its hybrid characteristic. Therefore, Preview module was used to set the list of variable modifications which were as follows: oxidation (M) as common and ammonia loss (N-term C), acetyl (protein N-term) and pyro-glutamination (protein N-term Q and protein N-term E) as rare modifications. Since, during MS^E experiments, all coeluting precursor ions are fragmented together, we increased the maximum number of precursors per MS^2 parameter to 10. The Excel reports were the input files for data aggregation carried out by Serac.[71]

2.3.3 | Determination of optimal CE setting using Serac

Energy dependence of peptides was investigated with the Byonic search engine. Byonic Excel reports were used as the input files for data aggregation carried out by our in-house developed program called Serac. Briefly, the program collected the identification scores (Byonic scores) as a function of CE from the energy-dependent mass spectrometric data series and determined the optimal CE. First, the Byonic scores were extracted from the Byonic Excel reports. Then, the score versus CE setting functions were normalized by dividing all values with the maximum score for the given identified peptide ion. To ensure that we draw conclusions on the basis of confident peptide identification, only peptide ions meeting certain minimum requirements were selected. First, we only considered a peptide identified at a given CE setting if its Byonic score exceeded 100. Furthermore, a peptide was included in the energy-dependent analysis if it was identified at least at six consecutive CE settings and for at least one CE it was found to have a Byonic score value above 300. For each peptide, the optimum CE was determined from the normalized score versus CE setting data sets by fitting Gaussian functions. For generating the nonlinear fits and the corresponding plots, the levmar[72] and PGPLOT[73] libraries were used through their Perl Data Language interface (see Material S1 for more details).

3 | RESULTS AND DISCUSSION

Our goal was to investigate the impact of the ion mobility separation on the optimal choice of CE setting on a Waters Select Series Cyclic IMS ion mobility mass spectrometer (see Figure 1) from the point of view of peptide identification. Further, we wanted to compare the pre- and post-ion mobility fragmentation possibilities. It is well known that CE markedly influences the list of fragment ions and their intensities in the MS/MS spectra, which form the basis of peptide identification in bottom-up proteomics. This is well illustrated by example spectra for $LAQANGWGVMVSHR^{3+}$ peptide taken on our instrument at three different CE activation in the transfer cell, which are depicted

in Figure 2. At low CE, namely at 15 V, the most intense peak is the parent ion, although some *b*- and *y*-type fragments are visible. Increasing the CE to 23 V results in nice *b* and *y* ion series allowing the sequence identification of the peptide. Finally, at the high 33 V CE, the more labile *b* ions disappear from the MS/MS spectrum, and some of the *y* ions are also subjected to further fragmentation processes.

Because ion heating occurs during IMS, the optimal CE providing the highest identification score may be different when IMS is applied. To address qualitatively and quantitatively this issue, four LC–MS/MS measurement series were carried out with systematically varied CE values: in two cases, the fragmentation was performed in the transfer cell either with IMS ($HDMS^E$) or without IMS (MS^E). In the other two cases, the trap cell was used for activation, again either with or without IMS. Tryptic peptides of HeLa standard were investigated, and 26 LC–MS/MS runs were acquired during each series of measurements. These belonged to 26 different CE values, providing score–CE curves, mapping the considered energy range in 2 V steps. When a given peptide was identified more than once in the same LC–MS/MS experiment, the best scoring match was accepted. Overall, we identified 6008, 6843 and 6587 peptides using the Byonic search engine in the case of transfer CID, transfer CID with IMS, and trap CID, respectively (see Table 1). Among these, 1175, 2063, and 1134, respectively, were considered sufficiently reliable to include in the energy-dependence analysis (see Data Analysis). In all cases, approximately

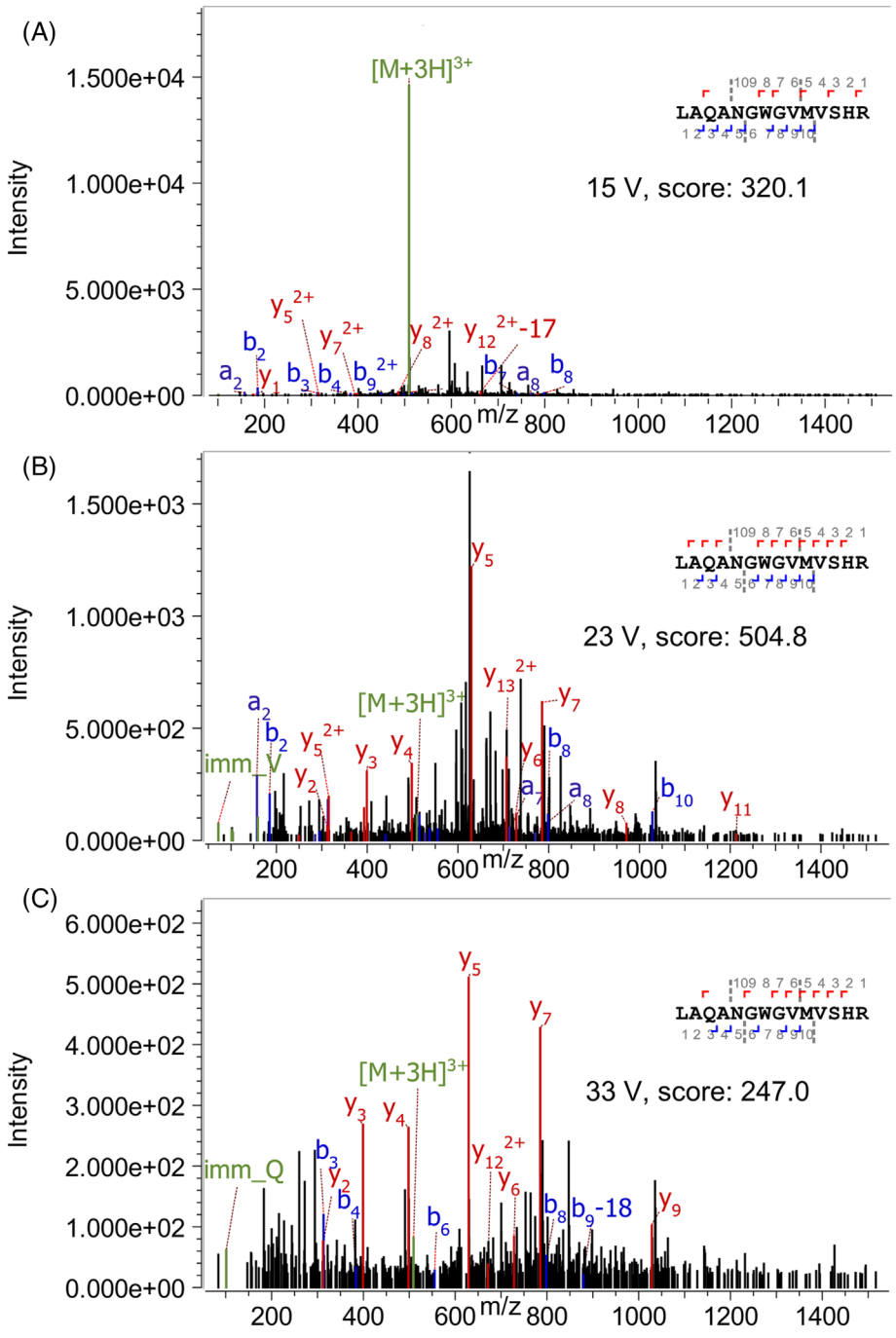

FIGURE 2 Selected MS/MS spectra of $LAQANGWGVMVSHR^{3+}$ peptide recorded on the Waters Cyclic IMS QTof instrument using transfer cell for fragmentation. Spectra were taken at three different collision energies, namely at (A) 15, (B) 23 V, and (C) 33 V. IMS, ion mobility spectrometry.

TABLE 1 Number of peptides with various properties for the different fragmentation modes.

	Transfer	TransferIMS	Trap
Identified from all runs (>100 score)	6008	6843	6587
Considered for energy dependence study	1175	2063	1134
From this, 2+	890	1650	820
From this, 3+	268	391	292
	Transfer and transferIMS		**Transfer and trap**
Peptides considered for energy dependence study and common between different series	1038		925
From this, 2+	835		706
From this, 3+	193		207

three quarters of these peptides were doubly charged, and most of the rest were triply charged.

From the number of identifications, it is obvious that the application of IMS is beneficial: there are almost twice as many hits in transfer CID with IMS compared to transfer CID. Data obtained from the measurements of trap cell with IMS were not interpretable, because there are less than a hundred peptide hits. The reason for this is when the CID in trap precedes the separation with ion mobility, fragment ions belonging to various peptides are mixed in the mobility region, after which the peptide identification by the database search becomes impossible. Therefore, we examined the influence of IMS with transfer CID, and we also compared the CE dependence of trap and transfer cells without ion mobility.

3.1 | Impact on individual peptides

First, we investigated how the score versus CE curves look like with and without ion mobility separation. We analyzed approximately 1000 peptides in the case of transfer CID and approximately 2000 peptides using transfer CID with IMS, and 1038 hits were common between the two sets of experiments. To illustrate the differences at the level of individual peptides, the energy dependence of Byonic scores for doubly protonated YSLEPVAVELK and triply protonated LAQANGWGVMVSHR peptides are depicted in Figure 3. Blue and red curves show the experimental points, whereas solid lines represent the results of Gaussian fitting. The CEs belonging to the maximum of the fitted curves were accepted as CE optimum values; they are denoted by crosses on the horizontal axes. As it can be seen, the optimum is at lower energy with the ion mobility separation in both cases by approximately 5 V. The optima are 19.2 and 24.8 V for the $YSLEPVAVELK^{2+}$ peptide and 17.9 and 22.6 V for the $LAQANGWGVMVSHR^{3+}$ peptide with and without IMS, respectively.

In average, across all common peptide hits, the CE optimum is 6.3 V lower for the case with IMS, and the effect does not differ significantly for the different charge states (see Figures S10 and S11). The histogram of the difference upon the use of IMS is shown in Figure 4. It can be seen that optimum CE decreases by 3–9 V for the majority of the peptides, and almost all (~90%) of the peptides have a downward shift in their CE optimum between 0 and 12 V upon the use of IMS. This clearly points out the existence of ion heating in the ion mobility cell and its relevance in bottom-up proteomics identifications. On the other hand, the manufacturer did not suggest taking this effect into account, implying the same recommended CE values regardless of the application of IMS. Our results indicate that the CE settings should be fine-tuned if we also perform ion mobility, because different—somewhat lower—settings may provide better performance.

As a next step, we compared the CE dependence of trap and transfer cells without ion mobility. The number of common peptides between the two sets of experiments was 925, and selected curves for two peptides are shown in Figure 3 as examples. The determined optimal CEs of the $YSLEPVAVELK^{2+}$ peptide are 24.8 and 30.4 V for the transfer CID and trap CID, respectively. Similar difference was found for the $LAQANGWGVMVSHR^{3+}$ peptide; the obtained optima are 22.6 and 30.4 V, respectively. On average, fragmentation in the trap cell was found to have an optimal setting greater by 7.2 V compared to the optimal voltage in the transfer cell. The distribution of the difference (see Figure S12) between optimal CEs in the trap and transfer cell shows that the maximum of the optimal CE increase is at 6–9 V, and ~90% of the peptides have a shift upward in the optimum CE between 3 and 12 V in the case of trap cell fragmentation compared to transfer cell activation. This indicates that the two collision cells do not have the same optimal CE setting, even though they are within the same device. This is in line with the literature where differences in optimal CE were found between similar instruments, and adjustments were necessary to obtain closely matching spectra.[48,74] Collision cells located at different parts of the same mass spectrometer may require different CE because ions enter them in somewhat different energetic conditions.

3.2 | Impact on trends

The previous section concluded that the optimal CE setting is lower for transfer CID with ion mobility than transfer CID without ion mobility. To investigate and compare the *m/z* dependent trends, as a next step, we plotted the optimum collision energies as a function of

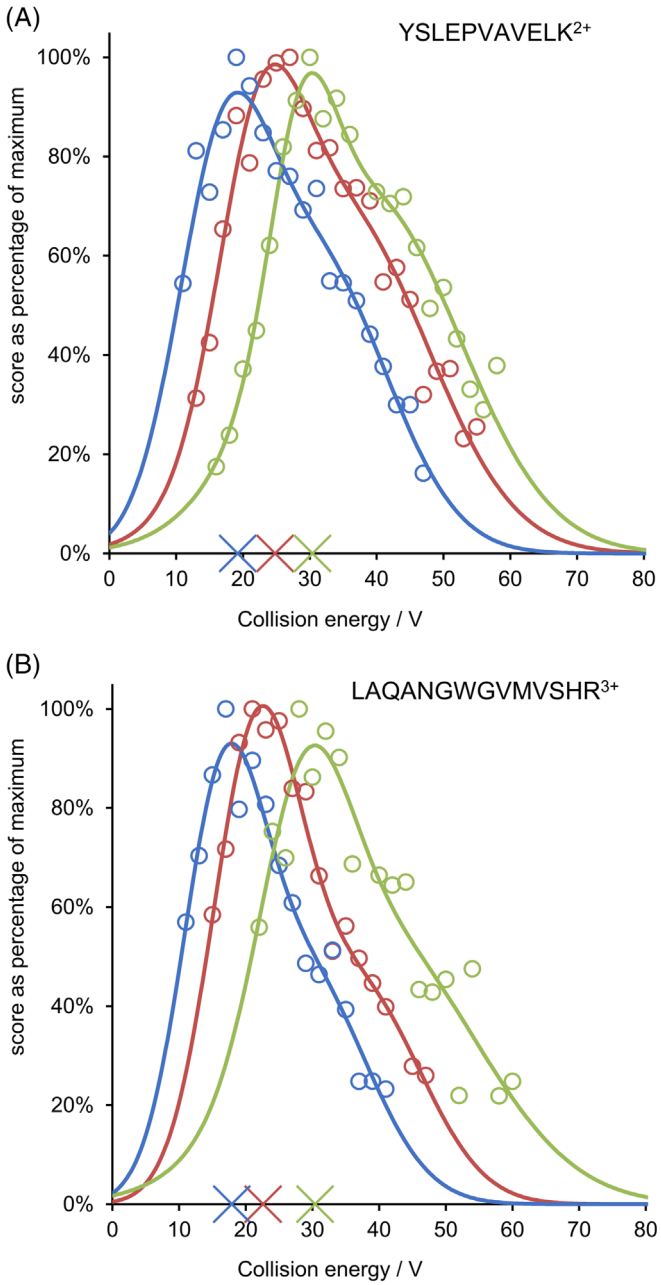

FIGURE 3 Result of fitting Gaussians to the energy-dependence data points (score as percent of the maximum value vs collision energy in V) of example peptides (A) YSLEPVAVELK^{2+} and (B) LAQANGWGVMVSHR^{3+}. Circles denote measured data, whereas solid lines depict the Gaussian model functions. The optimal CE is marked by crosses on the horizontal axis. Blue and red colors belong to fragmentation in the transfer cell with and without ion mobility, respectively. Green color shows results with fragmentation in the trap cell without IMS. IMS, ion mobility spectrometry; CE, collision energy.

the peptide ion *m/z* value (see Figure 5). The determined optimal CE values are represented by burgundy and blue circles belonging to the transfer CID and transfer CID with mobility, respectively. Apparently, the points follow the expected linear trends with respect to *m/z* for both cases with large variance. Inclusion of mobility separation shifts

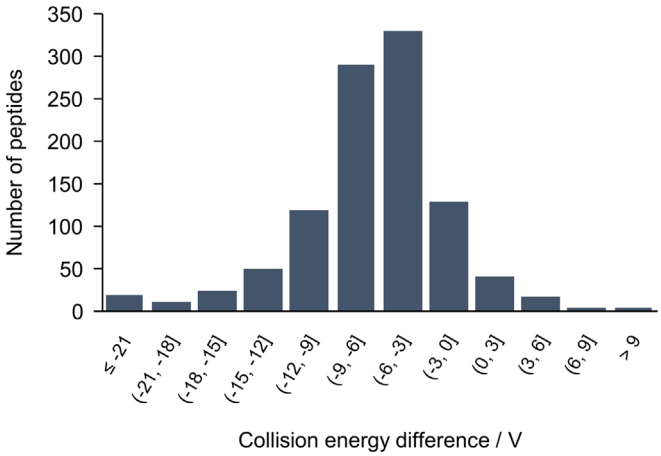

FIGURE 4 Distribution of optimal CE difference upon the use of ion mobility for the investigated peptides. CE, collision energy.

the trendline by ~4–10 V lower setting. Analysis on the subset of common peptides provided the same conclusion. Further, the above comparison was also carried out on the different charge states separately: although the trendlines are somewhat different, the obtained effect of the IMS was found similar (see Figures S13–S15). A closer examination of our data reveals that this shift is markedly higher for larger *m/z*. This suggests that peptides with larger collision cross section are energized more significantly.

Similar comparison was performed between the two CID cells of the QTof mass spectrometer (see Figure 6). As we concluded before, lower CE is optimal when fragmentation occurs in the transfer cell, but the trendlines have practically the same slope, meaning that the activation in the trap cell requires larger CE by ~7–10 V through the whole investigated *m/z* range. Again, data analysis on doubly and triply charged peptides separately and on peptides identified in both experimental series were carried out showing similar trends (see Figures S16–S18).

From another perspective, the impact of ion mobility separation can also be seen on the number of identified peptides at fixed collision energies. As shown in Figure 7, the maximum number of hits with transfer CID is increased to ~2500 from ~1400 upon turning on IMS. There was no significant difference between transfer and trap cell fragmentation (~1400 vs 1500 identifications at maximum). The results clearly show that the mobility separation boosts the performance of proteomics analysis. Further, the maximum number of identifications appear at ~27, 21, and 35 V in the case of transfer CID, transfer CID with mobility, and trap CID, respectively, which is again in line with the different optimal CE settings obtained above.

The number of identified peptides as a function of applied CE was also determined using PLGS search engine. Although the number of hits is somewhat different, the obtained trends are fully consistent with the Byonic results; even the CE values providing the highest number of peptides agree very well for the two search engines (see Figure S19).

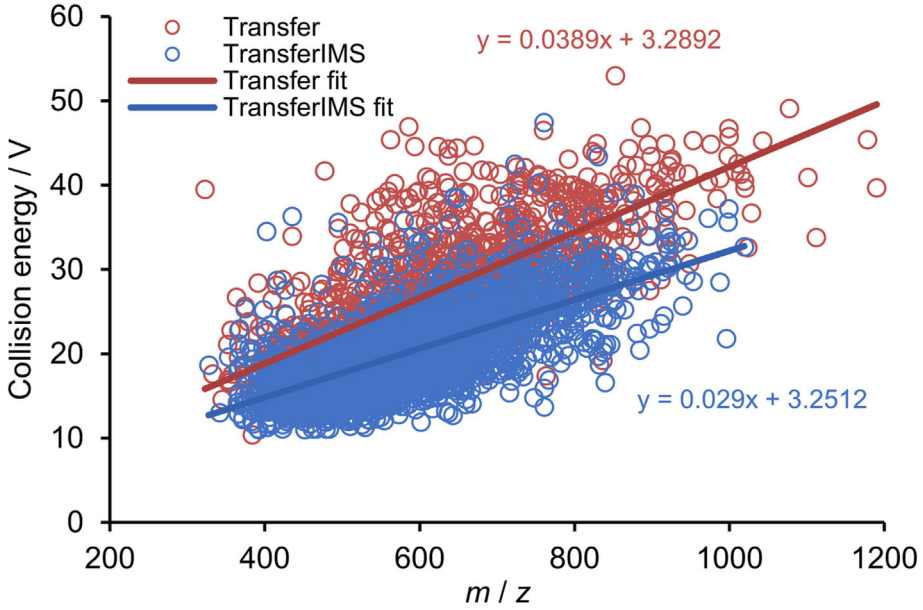

FIGURE 5 Optimal CE in V as a function of peptide *m/z* with activation in the transfer cell. Blue and burgundy circles indicate the optimum when IMS is applied and not applied, respectively. Solid lines represent linear fits to the experimental points. IMS, ion mobility spectrometry; CE, collision energy.

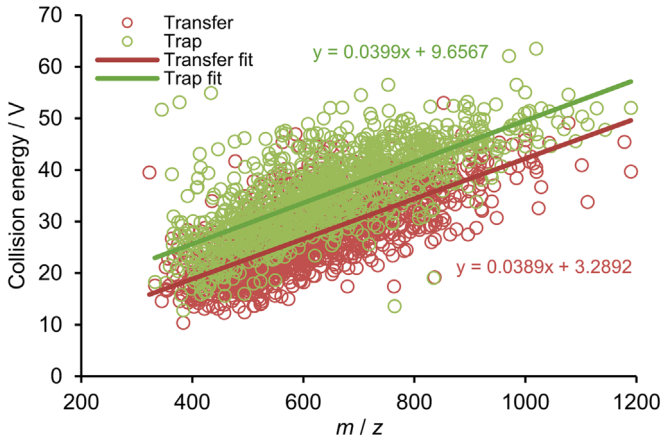

FIGURE 6 Optimal CE in V as a function of peptide *m/z* with activation in the transfer cell (burgundy) and trap cell (green). Circles depict measured optimum CE of peptides, while solid lines represent linear fits to the experimental points. CE, collision energy.

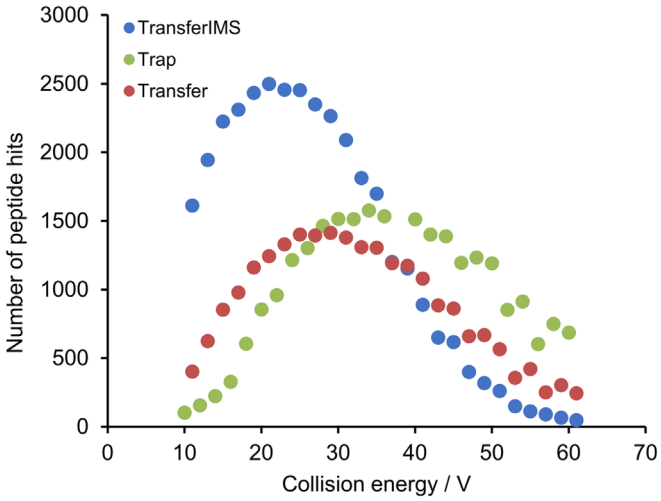

FIGURE 7 Number of peptide hits as a function of applied CE in V using 3 different experimental methods. Burgundy, blue, and green symbols belong to the transfer CID, transfer CID with IMS, and trap CID, respectively. IMS, ion mobility spectrometry; CE, collision energy; CID, collision-induced dissociation.

3.3 | Practical considerations

On our instrument, the manufacturer's recommended CE setting for proteomics is a ramp of 19–45 V in all ion fragmentation modes, both with and without IMS. How does this compare with the determined optimum CE values and *m/z* dependent trends? For transfer CID without IMS, we found that this range covers the optimum CE of most (~86%) of peptides, while 13% and 1% have lower and higher optimum, respectively. In contrast, when IMS is also applied, only 56% of peptides have optimum in the 19–45 V range, and as much as 44% of peptides can be identified with maximum score at a CE lower than 19 V. We would therefore expect improvement from adjusting the range when ion mobility separation is used; for example, with the use of a ramp between 12 and 34 V, 98% of the peptides would have their optima within the range, while the interval is still narrower than with the manufacturer's suggested setting. We highlight at this point that the optimal choice of experimental parameters is equipment dependent, because of the different extent of ion heating in various instruments. Specific optimization would be worth doing. Having the desired configuration for mobility separation in place is probably also important, because in the present project, we worked with one-cycle separation, and multiple cycles may supposedly have even larger impact. Further, if an instrument with data-dependent acquisition mode is used, it is even possible to apply an *m/z* dependent CE setting

or adjustment, which appears relevant because we saw that the influence of IMS on the trendlines is *m/z* dependent in an absolute sense. In that case, our determined linear fits can form the starting point to optimize a measurement protocol.

3.4 | Investigation of cyclic IMS settings influencing the observed ion heating

In the literature, it has already been highlighted that voltage settings of the cyclic IMS instrument may significantly influence ion transmission and activation for large biomolecular systems.[69] Correspondingly, we aimed to highlight cyclic IMS parameters that may have an impact on the observed peptide ion heating. To this end, we investigated the effect of several IMS settings on peptide fragmentation. Experimental series were performed on two diagnostic peptides by systematically changing various IMS parameters (see Material S2) while the other parameters were kept at the default values presented in Figures S1–S9). Analogous results were obtained for both investigated peptides: the increase of the TW static height, that of the separate array offset/racetrack bias or that of the post array bias voltages indeed have significant effect by activating ions resulting in increased fragment ion and decreased parent ion relative intensities (see Figure S20). The post array gradient and bias were tested together, and the influence of the post array bias voltage was observed at all of the investigated values of post array gradient. The other investigated parameters (namely the pre array gradient and bias, the inject array offset, and the separate time) had no or only slight influence on the relative intensities in the MS/MS spectra. Our data pinpoint how sensitively the magnitude of ion heating may change in response to adjusting some of the multitude of parameters of the intricate cyclic IMS device, making it essential to consider IMS parameter and CE optimization jointly in further applications.

4 | CONCLUSIONS

The phenomenon of ion heating because of the collisions with the buffer gas in the IMS cell is well-documented in the literature. Its effect on conformational changes of large molecules (e.g., proteins) and on the fragmentation processed of thermometer molecules was investigated by various research groups. But to our knowledge, this is the first study addressing this issue from the proteomics identification point of view. We performed systematic MS/MS measurements with varied CE settings on a large number of tryptic peptides from HeLa protein digest standard using a Waters Select Series Cyclic IMS QTof mass spectrometer. The experiments were carried out with and without IMS separation to obtain data in what extent IMS influences the optimal CE choice of bottom-up proteomics investigations. Further, the two CID fragmentation cell of the instrument, called trap cell and transfer cell, located ahead and behind the IMS cell, respectively, were compared. We found that IMS energizes the peptides significantly; therefore, the use of lower CE is advised when IMS is applied. The CE setting suggested by the manufacturer seemed optimal without IMS but proved to be quite off when IMS was on. Based on the results for more than 1000 peptides, we could formulate practical guidance for the optimal CE set. Further, CE adjustment is necessary when CID is performed in the trap cell instead of the transfer cell. Our results allowed us to the draw the following major conclusions:

1. Mobility has a notable impact on the CE for the highest score, which is also reflected in the optimum CE versus *m/z* trends. On average, peptides have an optimal CE at 6.3 V lower values upon IMS when one-cycle separation is applied.
2. Larger peptides are energized more resulting in larger difference in optima between with and without IMS for peptides having larger *m/z*.
3. Trap and transfer cells show some difference; fragmentation in the trap cell requires a few V higher CE value (7.2 V on average). The slope of CE versus *m/z* trendlines are practically identical. This observation is in line with the trends observed earlier for similar but not identical MS instruments.
4. Collision energy optimization is best carried out in the actual IM-MS configuration. CE adjustment is needed not only between the different CID fragmentation cells of the instrument but also some IMS parameters have significant effect on the activation and transmission, highlighting the importance of optimizing them jointly.

DATA AVAILABILITY STATEMENT

The data that support the findings of this study are openly available in MassIVE at https://doi.org/10.25345/C5HT2GH0Q, reference number MSV000090944.

ORCID

Gitta Schlosser https://orcid.org/0000-0002-7637-7133
Ágnes Révész https://orcid.org/0000-0002-6221-1239

REFERENCES

1. Lanucara F, Holman SW, Gray CJ, Eyers CE. The power of ion mobility-mass spectrometry for structural characterization and the study of conformational dynamics. *Nat Chem*. 2014;6(4):281-294. doi:10.1038/nchem.1889
2. Dodds JN, Baker ES. Ion mobility spectrometry: fundamental concepts, instrumentation, applications, and the road ahead. *J am Soc Mass Spectrom*. 2019;30(11):2185-2195. doi:10.1007/s13361-019-02288-2
3. Paglia G, Williams JP, Menikarachchi L, et al. Ion mobility derived collision cross sections to support metabolomics applications. *Anal Chem*. 2014;86(8):3985-3993. doi:10.1021/ac500405x
4. Kliman M, May JC, McLean JA. Lipid analysis and lipidomics by structurally selective ion mobility-mass spectrometry. *Biochim Biophys Acta - Mol Cell Biol Lipids*. 2011;1811(11):935-945. doi:10.1016/j.bbalip.2011.05.016
5. D'Atri V, Porrini M, Rosu F, Gabelica V. Linking molecular models with ion mobility experiments. Illustration with a rigid nucleic acid structure. *J Mass Spectrom*. 2015;50(5):711-726. doi:10.1002/jms.3590
6. Trimpin S, Clemmer DE. Ion mobility spectrometry/mass spectrometry snapshots for assessing the molecular compositions of complex polymeric systems. *Anal Chem*. 2008;80(23):9073-9083. doi:10.1021/ac801573n

7. Hanozin E, Mignolet B, Morsa D, et al. Where ion mobility and molecular dynamics meet to unravel the (un)folding mechanisms of an oligorotaxane molecular switch. *ACS Nano*. 2017;11(10):10253-10263. doi:10.1021/acsnano.7b04833
8. Hall Z, Politis A, Robinson CV. Structural modeling of heteromeric protein complexes from disassembly pathways and ion mobility-mass spectrometry. *Structure*. 2012;20(9):1596-1609. doi:10.1016/j.str.2012.07.001
9. Ruotolo BT, Benesch JLP, Sandercock AM, Hyung SJ, Robinson CV. Ion mobility-mass spectrometry analysis of large protein complexes. *Nat Protoc*. 2008;3(7):1139-1152. doi:10.1038/nprot.2008.78
10. Pringle SD, Giles K, Wildgoose JL, et al. An investigation of the mobility separation of some peptide and protein ions using a new hybrid quadrupole/travelling wave IMS/Oa-ToF instrument. *Int J Mass Spectrom*. 2007;261(1):1-12. doi:10.1016/j.ijms.2006.07.021
11. Massonnet P, Haler JRN, Upert G, et al. Ion mobility-mass spectrometry as a tool for the structural characterization of peptides bearing intramolecular disulfide bond(S). *J am Soc Mass Spectrom*. 2016;27(10):1637-1646. doi:10.1007/s13361-016-1443-8
12. Charkow J, Röst HL. Trapped ion mobility spectrometry reduces spectral complexity in mass spectrometry-based proteomics. *Anal Chem*. 2021;93(50):16751-16758. doi:10.1021/acs.analchem.1c01399
13. Cumeras R, Figueras E, Davis CE, Baumbach JI, Gràcia I. Review on ion mobility spectrometry. Part 1: current instrumentation. *Analyst*. 2015;140(5):1376-1390. doi:10.1039/c4an01100g
14. Haler JRN, Massonnet P, Chirot F, et al. Comparison of different ion mobility setups using poly (ethylene oxide) PEO polymers: drift tube, TIMS, and T-wave. *J am Soc Mass Spectrom*. 2018;29(1):114-120. doi:10.1007/s13361-017-1822-9
15. Oliinyk D, Meier F. Ion mobility-resolved phosphoproteomics with Dia-PASEF and short gradients. *Proteomics*. 2023;23:2200032. doi:10.1002/pmic.202200032
16. Skowronek P, Thielert M, Voytik E, et al. Rapid and in-depth coverage of the (Phospho-) proteome with deep libraries and optimal window design for Dia-PASEF. *Mol Cell Proteomics*. 2022;21(9):100279. doi:10.1016/j.mcpro.2022.100279
17. Meier F, Köhler ND, Brunner AD, et al. Deep learning the collisional cross sections of the peptide universe from a million experimental values. *Nat Commun*. 2021;12(1):1185. doi:10.1038/s41467-021-21352-8
18. Borotto NB, Osho KE, Richards TK, Graham KA. Collision-induced unfolding of native-like protein ions within a trapped ion mobility spectrometry device. *J am Soc Mass Spectrom*. 2022;33(1):83-89. doi:10.1021/jasms.1c00273
19. Morsa D, Gabelica V, De Pauw E. Fragmentation and isomerization due to field heating in traveling wave ion mobility spectrometry. *J am Soc Mass Spectrom*. 2014;25(8):1384-1393. doi:10.1007/s13361-014-0909-9
20. Shvartsburg AA, Smith RD. Fundamentals of traveling wave ion mobility spectrometry. *Anal Chem*. 2008;80(24):9689-9699. doi:10.1021/ac8016295
21. Michelmann K, Silveira JA, Ridgeway ME, Park MA. Fundamentals of trapped ion mobility spectrometry. *J am Soc Mass Spectrom*. 2015;26(1):14-24. doi:10.1007/s13361-014-0999-4
22. Kolakowski BM, Mester Z. Review of applications of high-field asymmetric waveform ion mobility spectrometry (FAIMS) and differential mobility spectrometry (DMS). *Analyst*. 2007;132(9):842-864. doi:10.1039/b706039d
23. Santiago BG, Campbell MT, Glish GL. Variables affecting the internal energy of peptide ions during separation by differential ion mobility spectrometry. *J am Soc Mass Spectrom*. 2017;28(10):2160-2169. doi:10.1007/s13361-017-1726-8
24. Morsa D, Gabelica V, De Pauw E. Effective temperature of ions in traveling wave ion mobility spectrometry. *Anal Chem*. 2011;83(14):5775-5782. doi:10.1021/ac201509p
25. Merenbloom SI, Flick TG, Williams ER. How hot are your ions in TWAVE ion mobility spectrometry? *J am Soc Mass Spectrom*. 2012;23(3):553-562. doi:10.1007/s13361-011-0313-7
26. Morsa D, Hanozin E, Eppe G, Quinton L, Gabelica V, Pauw ED. Effective temperature and structural rearrangement in trapped ion mobility spectrometry. *Anal Chem*. 2020;92(6):4573-4582. doi:10.1021/acs.analchem.9b05850
27. Eldrid C, Ujma J, Kalfas S, et al. Gas phase stability of protein ions in a cyclic ion mobility spectrometry traveling wave device. *Anal Chem*. 2019;91(12):7554-7561. doi:10.1021/acs.analchem.8b05641
28. Oranzi NR, Kemperman RHJ, Wei MS, et al. Measuring the integrity of gas-phase conformers of sodiated 25-hydroxyvitamin D3 by drift tube, traveling wave, trapped, and high-field asymmetric ion mobility. *Anal Chem*. 2019;91(6):4092-4099. doi:10.1021/acs.analchem.8b05723
29. Ieritano C, Featherstone J, Haack A, Guna M, Campbell JL, Hopkins WS. How hot are your ions in differential mobility spectrometry? *J am Soc Mass Spectrom*. 2020;31(3):582-593. doi:10.1021/jasms.9b00043
30. Harrison JA, Kelso C, Pukala TL, Beck JL. Conditions for analysis of native protein structures using uniform field drift tube ion mobility mass spectrometry and characterization of stable calibrants for TWIM-MS. *J am Soc Mass Spectrom*. 2019;30(2):256-267. doi:10.1007/s13361-018-2074-z
31. Mwangi JN, Todd DA, Chiu NHL. Evaluating the variation of ion energy under different parameter settings in traveling wave ion mobility mass spectrometry. *Int J Ion Mobil Spectrom*. 2018;21(3):81-86. doi:10.1007/s12127-018-0238-y
32. Naylor CN, Ridgeway ME, Park MA, Clowers BH. Evaluation of trapped ion mobility spectrometry source conditions using benzylammonium thermometer ions. *J am Soc Mass Spectrom*. 2020;31(7):1593-1602. doi:10.1021/jasms.0c00151
33. Bleiholder C, Liu FC, Chai M. Comment on effective temperature and structural rearrangement in trapped ion mobility spectrometry. *Anal Chem*. 2020;92(24):16329-16333. doi:10.1021/acs.analchem.0c02052
34. Borotto NB, Graham KA. Fragmentation and mobility separation of peptide and protein ions in a trapped-ion mobility device. *Anal Chem*. 2021;93(29):9959-9964. doi:10.1021/acs.analchem.1c01188
35. Gabelica V, Livet S, Rosu F. Optimizing native ion mobility Q-TOF in helium and nitrogen for very fragile noncovalent structures. *J am Soc Mass Spectrom*. 2018;29(11):2189-2198. doi:10.1007/s13361-018-2029-4
36. Morsa D, Hanozin E, Gabelica V, De Pauw E. Response to comment on effective temperature and structural rearrangement in trapped ion mobility spectrometry. *Anal Chem*. 2020;92(24):16334-16337. doi:10.1021/acs.analchem.0c03937
37. Ieritano C, Rickert D, Featherstone J, et al. The charge-state and structural stability of peptides conferred by microsolvating environments in differential mobility spectrometry. *J am Soc Mass Spectrom*. 2021;32(4):956-968. doi:10.1021/jasms.0c00469
38. Lermyte F, Sobott F. A broader view on ion heating in traveling-wave devices using fragmentation of CsI clusters and extent of H migration as molecular thermometers. *Analyst*. 2017;142(18):3388-3399. doi:10.1039/c7an00161d
39. Révész Á, Rokob TA, Jeanne Dit Fouque D, et al. Selection of collision energies in proteomics mass spectrometry experiments for best peptide identification: study of mascot score energy dependence reveals double optimum. *J Proteome Res*. 2018;17(5):1898-1906. doi:10.1021/acs.jproteome.7b00912
40. Révész Á, Milley MG, Nagy K, et al. Tailoring to search engines: bottom-up proteomics with collision energies optimized for

identification confidence. *J Proteome Res*. 2021;20(1):474-484. doi:10.1021/acs.jproteome.0c00518

41. Riley NM, Malaker SA, Driessen MD, Bertozzi CR. Optimal dissociation methods differ for N- and O-glycopeptides. *J Proteome Res*. 2020;19(8):3286-3301. doi:10.1021/acs.jproteome.0c00218
42. Hinneburg H, Stavenhagen K, Schweiger-Hufnagel U, et al. The art of destruction: optimizing collision energies in quadrupole-time of flight (Q-TOF) instruments for glycopeptide-based glycoproteomics. *J am Soc Mass Spectrom*. 2016;27(3):507-519. doi:10.1007/s13361-015-1308-6
43. Yang H, Yang C, Sun T. Characterization of Glycopeptides using a stepped higher-energy C-trap dissociation approach on a hybrid quadrupole Orbitrap. *Rapid Commun Mass Spectrom*. 2018;32(16):1353-1362. doi:10.1002/rcm.8191
44. Hevér H, Nagy K, Xue A, et al. Diversity matters: optimal collision energies for tandem mass spectrometric analysis of a large set of N-glycopeptides. *J Proteome Res*. 2022;21(11):2743-2753. doi:10.1021/acs.jproteome.2c00519
45. Diedrich JK, Pinto AFM, Yates JR. Energy dependence of HCD on peptide fragmentation: stepped collisional energy finds the sweet spot. *J am Soc Mass Spectrom*. 2013;24(11):1690-1699. doi:10.1007/s13361-013-0709-7
46. Steckel A, Révész Á, Papp D, Uray K, Drahos L, Schlosser G. Stepwise collision energy-resolved tandem mass spectrometric experiments for the improved identification of citrullinated peptides. *J am Soc Mass Spectrom*. 2022;33(7):1176-1186. doi:10.1021/jasms.2c00031
47. Zolg DP, Wilhelm M, Schmidt T, et al. Proteometools: systematic characterization of 21 post-translational protein modifications by liquid chromatography tandem mass spectrometry (LC-MS/MS) using synthetic peptides. *Mol Cell Proteomics*. 2018;17(9):1850-1863. doi:10.1074/mcp.TIR118.000783
48. Szabó D, Schlosser G, Vékey K, Drahos L, Révész Á. Collision energies on QTof and Orbitrap instruments: how to make proteomics measurements comparable? *J Mass Spectrom*. 2021;56(1):e4693. doi:10.1002/jms.4693
49. Révész Á, Hevér H, Steckel A, et al. Collision energies: optimization strategies for bottom-up proteomics. *Mass Spectrom Rev*. 2021;42(4):e21763. doi:10.1002/mas.21763
50. Giles K, Ujma J, Wildgoose J, et al. A cyclic ion mobility-mass spectrometry system. *Anal Chem*. 2019;91(13):8564-8573. doi:10.1021/acs.analchem.9b01838
51. Delafield DG, Lu G, Kaminsky CJ, Li L. High-end ion mobility mass spectrometry: a current review of analytical capacity in omics applications and structural investigations. *TrAC - Trends Anal Chem*. 2022;157:116761. doi:10.1016/j.trac.2022.116761
52. Rüger CP, Le Maître J, Riches E, et al. Cyclic ion mobility spectrometry coupled to high-resolution time-of-flight mass spectrometry equipped with atmospheric solid analysis probe for the molecular characterization of combustion particulate matter. *J am Soc Mass Spectrom*. 2021;32(1):206-217. doi:10.1021/jasms.0c00274
53. Snyder DT, Jones BJ, Lin YF, et al. Surface-induced dissociation of protein complexes on a cyclic ion mobility spectrometer. *Analyst*. 2021;146(22):6861-6873. doi:10.1039/d1an01407b
54. McKenna KR, Li L, Baker AG, et al. Carbohydrate isomer resolution: via multi-site derivatization cyclic ion mobility-mass spectrometry. *Analyst*. 2019;144(24):7220-7226. doi:10.1039/c9an01584a
55. Ropartz D, Fanuel M, Ujma J, Palmer M, Giles K, Rogniaux H. Structure determination of large isomeric oligosaccharides of natural origin through multipass and multistage cyclic traveling-wave ion mobility mass spectrometry. *Anal Chem*. 2019;91(18):12030-12037. doi:10.1021/acs.analchem.9b03036
56. Zöller J, Hong S, Eisinger ML, et al. Ligand binding and conformational dynamics of the E. Coli nicotinamide nucleotide transhydrogenase revealed by hydrogen/deuterium exchange mass spectrometry. *Comput Struct Biotechnol J*. 2022;20:5430-5439. doi:10.1016/j.csbj.2022.09.036
57. Tomczyk N, Giles K, Richardson K, et al. Mapping isomeric peptides derived from biopharmaceuticals using high-resolution ion mobility mass spectrometry. *Anal Chem*. 2021;93(49):16379-16384. doi:10.1021/acs.analchem.1c02834
58. Deslignière E, Botzanowski T, Diemer H, et al. High-resolution IMS-MS to assign additional disulfide bridge pairing in complementarity-determining regions of an IgG4 monoclonal antibody. *J am Soc Mass Spectrom*. 2021;32(10):2505-2512. doi:10.1021/jasms.1c00151
59. Kováč A, Majerová P, Nytka M, et al. Separation of isomeric tau phosphopeptides from Alzheimer's disease brain by cyclic ion mobility mass spectrometry. *J am Soc Mass Spectrom*. 2023;34(3):394-400. doi:10.1021/jasms.2c00289
60. Gibson K, Cooper-Shepherd DA, Pallister E, Inman SE, Jackson SE, Lindo V. Toward rapid aspartic acid isomer localization in therapeutic peptides using cyclic ion mobility mass spectrometry. *J am Soc Mass Spectrom*. 2022;33(7):1204-1212. doi:10.1021/jasms.2c00053
61. Oganesyan I, Hajduk J, Harrison JA, Marchand A, Czar MF, Zenobi R. Exploring gas-phase MS methodologies for structural elucidation of branched N-glycan isomers. *Anal Chem*. 2022;94(29):10531-10539. doi:10.1021/acs.analchem.2c02019
62. Sanda M, Morrison L, Goldman R. N-and O-glycosylation of the SARS-CoV-2 spike protein. *Anal Chem*. 2021;93(4):2003-2009. doi:10.1021/acs.analchem.0c03173
63. Sisley EK, Ujma J, Palmer M, Giles K, Fernandez-Lima FA, Cooper HJ. LESA cyclic ion mobility mass spectrometry of intact proteins from thin tissue sections. *Anal Chem*. 2020;92(9):6321-6326. doi:10.1021/acs.analchem.9b05169
64. Shaw JB, Cooper-Shepherd DA, Hewitt D, et al. Enhanced top-down protein characterization with electron capture dissociation and cyclic ion mobility spectrometry. *Anal Chem*. 2022;94(9):3888-3896. doi:10.1021/acs.analchem.1c04870
65. Deslignière E, Ollivier S, Beck A, Ropartz D, Rogniaux H, Cianférani S. Benefits and limitations of high-resolution cyclic IM-MS for conformational characterization of native therapeutic monoclonal antibodies. *Anal Chem*. 2023;95(8):4162-4171. doi:10.1021/acs.analchem.2c05265
66. Deslignière E, Ollivier S, Ehkirch A, et al. Combination of IM-based approaches to unravel the coexistence of two conformers on a therapeutic multispecific MAb. *Anal Chem*. 2022;94(22):7981-7989. doi:10.1021/acs.analchem.2c00928
67. Al-jabiry A, Palmer M, Langridge J, Bellamy-Carter J, Robinson D, Oldham NJ. Combined chemical modification and collision induced unfolding using native ion mobility-mass spectrometry provides insights into protein gas-phase structure. *Chem - a Eur J*. 2021;27(55):13783-13792. doi:10.1002/chem.202101857
68. Eldrid C, Ben-Younis A, Ujma J, et al. Cyclic ion mobility-collision activation experiments elucidate protein behavior in the gas phase. *J am Soc Mass Spectrom*. 2021;32(6):1545-1552. doi:10.1021/jasms.1c00018
69. Zenobi R, Harrison JA, Pruška A, Bittner P, Muck A, Cooper-Shepherd DA. Advancing cyclic ion mobility mass spectrometry methods for studying biomolecules: toward the conformational dynamics of mega Dalton protein aggregates. *Anal Chem*. 2022;94(36):12435-12443. doi:10.1021/acs.analchem.2c02406
70. Corasolla Carregari V, Monforte M, Di Maio G, et al. Proteomics of muscle microdialysates identifies potential circulating biomarkers in facioscapulohumeral muscular dystrophy. *Int J Mol Sci*. 2021;22(1):290. doi:10.3390/ijms22010290
71. Révész Á, Rokob TA, Jeanne Dit Fouque D, et al. Optimal collision energies and bioinformatics tools for efficient bottom-up sequence

validation of monoclonal antibodies. *Anal Chem*. 2019;91(20): 13128-13135. doi:10.1021/acs.analchem.9b03362

72. Lourakis MI, Levmar A. *Levenberg-Marquardt nonlinear least squares algorithms in C/C++, version 2.6*. Institute of Computer Science, Foundation for Research and Technology – Hellas. http://www.ics.forth.gr/~lourakis/levmar/2011
73. Pearson T. *PGPLOT 5.2.2*. California Institute of Technology. http://www.astro.caltech.edu/~tjp/pgplot/2001
74. Bazsó FL, Ozohanics O, Schlosser G, Ludányi K, Vékey K, Drahos L. Quantitative comparison of tandem mass spectra obtained on various instruments. *J am Soc Mass Spectrom*. 2016;27(8):1357-1365. doi:10.1007/s13361-016-1408-y

SUPPORTING INFORMATION

Additional supporting information can be found online in the Supporting Information section at the end of this article.

How to cite this article: Nagy K, Gellén G, Papp D, Schlosser G, Révész Á. Optimum collision energies for proteomics: The impact of ion mobility separation. *J Mass Spectrom*. 2023;58(9):e4957. doi:10.1002/jms.4957